

**Spiers Memorial Lecture
On Dynamics
From isolated molecules to biomolecules**

Joshua Jortner

School of Chemistry, Tel Aviv University, Ramat Aviv, 69978 Tel Aviv, Israel

We address the dynamics of electronic–vibrational excited states in isolated molecules, clusters, condensed phase and biosystems, which pertain to the phenomena of energy acquisition, storage and disposal as explored from the microscopic point of view. The advent of femtosecond dynamics opened up new horizons in the exploration of chemical and biophysical processes on the timescale of nuclear motion. These ultrafast radiationless processes involve isolated molecules, where ultrafast ‘nonreactive’ intramolecular internal conversion can occur on the timescale of vibrational motion, while ‘reactive’ dissociation and Coulomb explosion manifest the sliding down on the repulsive nuclear surface. In some cluster and condensed phase systems ultrafast energy dissipation processes, manifesting collective large nuclear configurational changes, bear analogy to the molecular ‘reactive’ dynamics, but can concurrently maintain vibrational phase coherence induced by nuclear impact. For ultrafast dynamics in clusters, in the condensed phase and in the protein medium, separation of timescales for nuclear dynamics may prevail. Interstate and energy relaxation are understood, while the interplay between relaxation and dephasing is of considerable interest. The ubiquity of vibrational and electronic coherence effects, ranging from small to huge systems, raises the conceptual question of the distinction between the experimental conditions of the preparation and interrogation, and the intrinsic aspects of relaxation and dephasing dynamics. These are some of the central aspects of the novel and fascinating area of femtosecond chemistry, whose conceptual framework rests on a unified theory and simulation of intramolecular, cluster, condensed phase and biophysical dynamics.

It is an honor to deliver the 1997 Spiers Memorial Lecture. Frederick S. Spiers left his mark on the scientific infrastructure of physical chemistry, as secretary of the Faraday Society, which he helped to found in 1902. Essentially, he has determined the character of these scientific discussions by which the Faraday Society and later the Faraday Division of the Royal Society of Chemistry became famous throughout the world. The interests of Spiers transcended pure and applied chemistry, encompassing music and culture. He was a fine Hebrew and Talmudic scholar. At the onset of the Spiers Memorial Lecture on Dynamics, it may be appropriate to quote from an old Hebrew scholarship: ‘You should know where you are coming from and where you are going to’, Proceedings of the Sage Fathers, 2nd Century AD. This quotation captures the essence of dynamics from isolated molecules to biomolecules, pertaining to the elucidation of the phenomena of energy acquisition, storage and disposal in large molecules, clusters, condensed phase and biophysical systems, as explored from the microscopic point of view.

The genesis of intramolecular nonradiative dynamics dates back to the origins of quantum mechanics. In 1928 Bonhoeffer and Farkas¹ observed that predissociation of

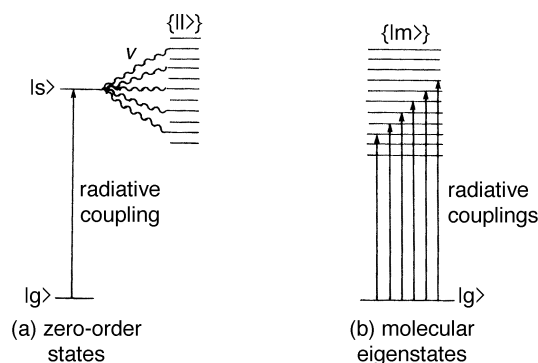


Fig. 1 A molecular energy-level model used to describe coupling and nonreactive relaxation in a bound-level structure in excited states of large molecules. This model was introduced by Bixon and Jortner^{18,19} to describe interstate coupling and relaxation, and is adequate to describe intrastate coupling and intramolecular vibrational energy redistribution.

the ammonia molecule is manifested by spectral line broadening (line width Γ). This observation established experimental verification of the Heisenberg energy–time uncertainty relation $\Gamma\tau \approx \hbar$, with the decay lifetime of the metastable state being given by the golden rule² $\tau^{-1} \propto |H|^2(dn/dE)$, where H is the matrix element of the perturbation causing the transition, and dn/dE is the energy density of states. The same formalism was concurrently applied for atomic and molecular autoionization.² The studies of predissociation and autoionization established the conceptual framework of the dynamics and the dynamic–spectroscopic relations for the decay of a metastable state into a (dissociative or ionizative) continuum. Important developments in the realm of intermolecular dynamics were pioneered by Wigner, Polanyi and Eyring in the 1930s,³ for kinetics in the gas phase, in molecular beams and in solution.⁴ In the 1950s and 1960s the conceptual framework was advanced for two novel classes of nonradiative process, *i.e.*, dynamics in the condensed phase and intramolecular radiationless transitions in large molecules. The field of nonradiative dynamics in the condensed phase was pioneered by Huang and Rhys,⁵ Kubo,⁶ Lax,⁷ and Kubo and Toyozawa⁸ in the context of the theory of electron–hole recombination in semiconductors. Conceptually and physically isomorphous classes of radiationless phenomena pertain to the theoretical foundations of electron transfer (ET) processes in solution, whose exploration was pioneered by Marcus,⁹ and electronic energy transfer (EET) processes, which were elucidated by Förster.¹⁰ When this significant progress was accomplished in the 1950s, no one realized the interrelationship between condensed-matter relaxation, *e.g.*, electron–hole recombination, electron transfer and energy transfer, and intramolecular radiationless transitions, *e.g.*, intersystem crossing and internal conversion in large molecules. At that time some experimental information was already available on intramolecular relaxation in large molecules embedded in a condensed medium, *i.e.*, a solution or a glass. Kasha formulated his (approximate) rules to characterize internal conversion and intersystem crossing of solvated organic molecules,¹¹ while Beer and Longuet-Higgins provided striking experimental evidence for the internal conversion of the first singlet excited state of azulene in solution.¹² Guided by the experimental background, the first theories of relaxation of large molecules focused on the coupling to the medium as an essential ingredient inducing electronic–vibrational conversion. Robinson and Frosch¹³ proposed sequential interstate electronic coupling and medium-induced vibrational relaxation, Gouterman¹⁴ alluded to medium phonon emission, while Lin¹⁵ and Lin and Bersohn¹⁶ considered medium and intramolecular multiphonon processes. A central ingredient of electronic relaxation in large molecules originated from the seminal experiments of

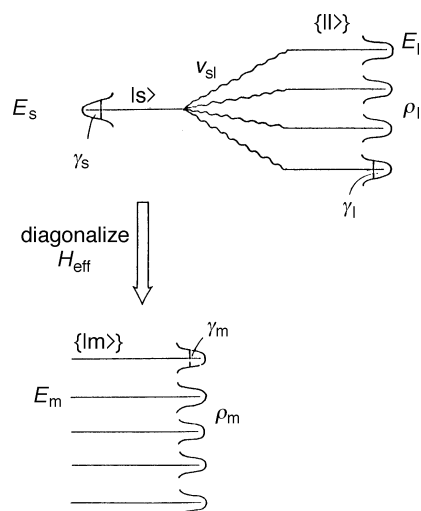


Fig. 2 The application of the effective Hamiltonian formalism for interstate and intrastate intramolecular coupling and dynamics. The zero-order states $|s\rangle$ and $\{l\rangle\}$ are characterized by the energies E_s and $\{E_l\}$, respectively, and by the decay widths γ_s and $\{\gamma_l\}$. V_{sl} represents the intramolecular (interstate or intrastate) coupling between the doorway state $|s\rangle$ and the $\{l\rangle\}$ manifold, which is characterized by the density of states ρ_l . Diagonalization of the effective Hamiltonian results in a set of independently decaying levels $\{m\rangle\}$, *i.e.*, generalized molecular eigenstates, characterized by energies $\{E_m\}$, decay widths $\{\gamma_m\}$, and density of states ρ_m .

Kistiakowski and Parmenter, which demonstrated the occurrence of intersystem crossing in the ‘isolated’ collision-free benzene molecule.¹⁷ The iconoclastic implications of the occurrence of irreversible relaxation in a bound level structure were fully realized by Kistikowski and Parmenter, who stated that their results may be incompatible with the laws of quantum mechanics.¹⁷ The intramolecular nature of radiationless transitions in a bound level structure was established by the Bixon–Jortner model,^{18–25} which rests on near-resonance coupling, the dynamics of wavepackets of mixed bound states, finite time evolution, and practical irreversibility in a dense bound level structure of a vibrational quasicontinuum (Fig. 1). This general conceptual framework is applicable both for interstate coupling,^{18–36} which involves two electronic configurations coupled by nuclear momenta (*i.e.*, the breakdown of the Born–Oppenheimer separability), and/or spin–orbit interaction, as well as for intrastate coupling, which involves intramolecular vibrational energy redistribution (IVR) within a single electronic configuration with rotational–vibrational states coupled by anharmonic or Coriolis interactions.^{35,36} This theoretical framework is of wide applicability for the exploration of the dynamics of electronically excited states of ‘isolated’ molecules in the gas phase, of clusters, and in condensed media.

Femtosecond dynamics opened up new horizons in the exploration of ultrafast radiationless processes. In the realm of chemical and biological dynamics ultrafast relaxation can prevail on the timescale of nuclear motion. The exploration of ultrafast chemical and biological dynamics stems from concurrent progress in theory and experiment. The advent of fs lasers allows for the real-time interrogation of the intramolecular and intermolecular nuclear motion during chemical and biophysical transformation.^{37–39} On the theoretical front, the theory and simulations of radiationless processes,^{40,41} wavepacket dynamics,⁴² coherence effects,⁴² cluster dynamic size effects,⁴³ nonadiabatic condensed phase dynamics^{40,41} and nonlinear optical interactions⁴⁴ provide the conceptual framework for ultrafast intramolecular, cluster, condensed phase and biophysical dynamics.

Classification of level structure

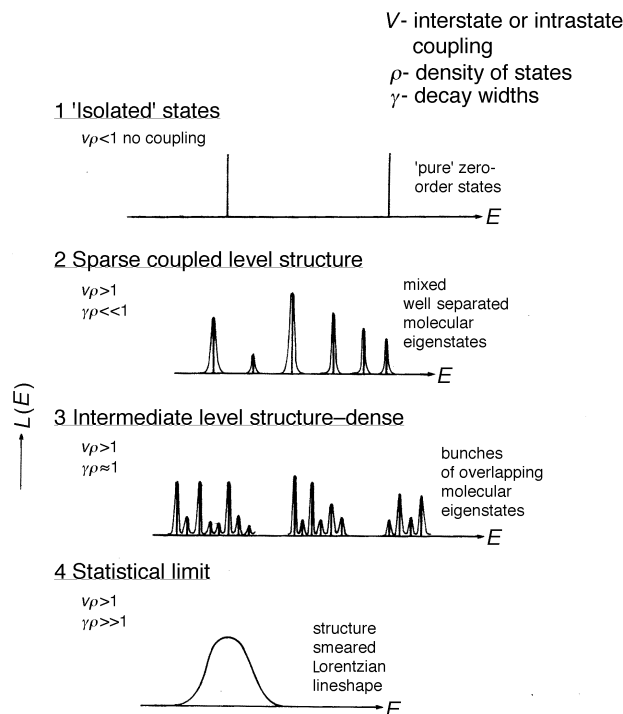


Fig. 3 Classification of the intramolecular level structure. The relevant energetic and dynamic parameters are: the (interstate and intrastate) coupling V , the density of the independently decaying levels ρ and their decay widths γ . The spectra exhibit the energy dependent line-shapes $L(E)$ vs. E .

Intramolecular dynamics in a bound level structure

The central ingredients of the theory of intramolecular dynamics in a bound level structure, developed by Bixon, Nitzan, Mukamel and Jortner,^{26–36,45,46} are as follows:

(1) The characterization of the level structure. This requires the characterization of the appropriate zero-order states and their (small) couplings.

(2) The accessibility of the zero-order states, leading to the specification of the doorway state(s) of the system.

(3) The decay channels of the zero-order states, specifying their decay to genuine (radiative decay, predissociation, autoionization) continuum channels, which are characterized by appropriate decay widths.

(4) The initial excitation conditions, which are governed by the (optical) excitation modes.

Ingredients (1) and (3) allow for the construction of the (complex) molecular eigenstates, *i.e.*, the independently decaying molecular levels $\{|m\rangle\}$, which are obtained from the diagonalization of the effective Hamiltonian^{26–36,45,46}

$$\hat{H}_{\text{eff}} = \hat{H}_{\text{M}} - (i/2)\hat{\Gamma} \quad (1)$$

where \hat{H}_{M} is the molecular Hamiltonian and $\hat{\Gamma}$ is the decay matrix (Fig. 2). The $\{|m\rangle\}$ states are characterized by the complex energies

$$\varepsilon_m = E_m - (i/2)\gamma_m \quad (2)$$

where $\{E_m\}$ are the energy levels, while $\{\gamma_m\}$ represents the decay widths. Relevant time-resolved observables for a broad-band excitation, which are based on ingredients (1) and (2), involve the population probability of the doorway state

$$P^{(D)}(t) = \left| \sum_m |A_m|^2 \exp\left(-\frac{iE_m t}{\hbar} - \frac{\gamma_m t}{2\hbar}\right) \right|^2 \quad (3)$$

where $A_m = \langle g | \hat{\mu} | m \rangle$ are the excitation amplitudes of the $\{|m\rangle\}$ manifold, and the energy-resolved (radiative) decay probability to a vibrational level $|gv\rangle$ of the ground electronic state

$$P^{(v)}(t) = \left| \sum_m A_m B_m^v \exp\left(\frac{-iE_m t}{\hbar} - \frac{\gamma_m t}{2\hbar}\right) \right|^2 \quad (4)$$

where $B_m^v = \langle m | \hat{\mu} | gv \rangle$ are the transition amplitudes. These probabilities constitute Fourier sums damped by real decay exponents, and may involve either a superposition of exponentials (for a sparse or intermediate level structure) or an exponential decay of a giant resonance (in the statistical limit), while eqn. (4) may also result in quantum beats (in the intermediate level structure). The character and dynamical manifestations of the sparse, intermediate and statistical level structure (Fig. 3) can be inferred in a transparent way from the lineshapes $L(E) = -\text{Im}G(E)$, where the Green's function is $G(E) = (E - H_{\text{eff}})^{-1}$. The classification of the level structures (Fig. 3) is specified by the coarse grained interstate or intrastate coupling V , by the density of states of the proper symmetry ρ , and by the decay widths γ . The limit of isolated states, with $V\rho < 1$, constitutes the spectroscopist's paradise, when distinct 'pure' rotational-vibrational levels can be observed. For the strongly coupled situation, with $V\rho > 1$, the sparse ($\gamma\rho < 1$), the intermediate ($\gamma\rho \approx 1$) and the statistical ($\gamma\rho \gg 1$) level structures (Fig. 3), can be realized.

The statistical limit, mode selectivity and vibronic and electronic chemistry

Some aspects of the theory and experiment relevant to dynamics in isolated molecules will now be addressed.

A Ultrafast intramolecular relaxation in the statistical limit

The statistical limit corresponds to the extreme situation of overlapping resonances, where the whole structure in the spectrum is washed out (Fig. 3). The absorption lineshape is Lorentzian with the width $\Gamma = 2\pi \sum_i |V_{si}|^2 \delta(E_s - E_i)$ and the nonradiative lifetime $\tau = \hbar/\Gamma$. These predictions were confirmed in the 1980s by the experimental observation of a Lorentzian absorption lineshape due to internal conversion from the electronic origin (which precludes IVR) of some intravalence excitations of large isolated jet-cooled molecules,⁴⁷⁻⁵¹ e.g., the S_1 origin of azulene (Fig. 4) and the S_2 origin (Q_y band) of free base porphyrin (Fig. 5), as well as of the extravalence Rydberg excitations (principal quantum number $n = 3-5$) of benzene (Fig. 6). The observation of a Lorentzian lineshape for a highly congested bound level structure constitutes the victory of dynamics over spectroscopy. The spectroscopic information (Table 1) on ultrafast dynamics ($\tau = 3000-10$ fs) reveals that the timescale for internal conversion of high intravalence excitations of benzene and anthracene (10-20 fs) corresponds to the highest molecular vibrational frequencies $1500-3000 \text{ cm}^{-1}$. Only recently the first time-resolved lifetime of ca. 40 fs for the S_2 state of isolated benzene was reported by Hertel and co-workers.^{52a} It is an open question whether these ultrafast relaxation times in high electronic excitations of large, rigid aromatics correspond to the weak coupling limit or to the strong coupling limit, according to the Englman-Jortner classification.⁵³ The

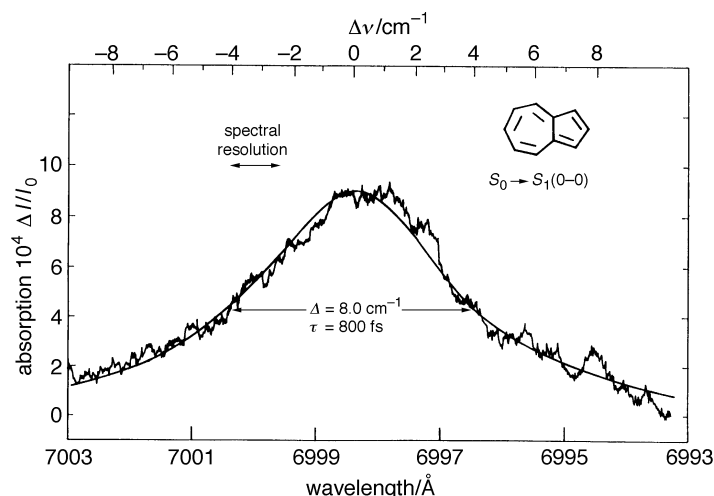


Fig. 4 The absorption spectrum of the 0-0 electronic origin of the $S_0 \rightarrow S_1$ of the isolated jet-cooled azulene molecule ($T_{\text{rot}} = 20$ K, $T_{\text{vib}} = 30$ K). The Lorentzian line broadening (fitted by a solid line) reflects intramolecular coupling and statistical limit $S_1(0-0) \rightarrow S_0^*$ relaxation in a bound level structure (ref. 47).

strong coupling limit, where the two potential energy surfaces cross in the vicinity of the minimum of the higher surface, and which may also include the situation of conical intersection under proper symmetry representation,⁵⁴ can be realized for some intramolecular isomerization processes and for some cases of intermolecular coupling to exterior medium modes. In the weak coupling limit the displacement of the minima of the two surfaces is small so that the dynamics occurs in the region where no surface crossing prevails. This state of affairs bears analogy to nuclear tunneling.

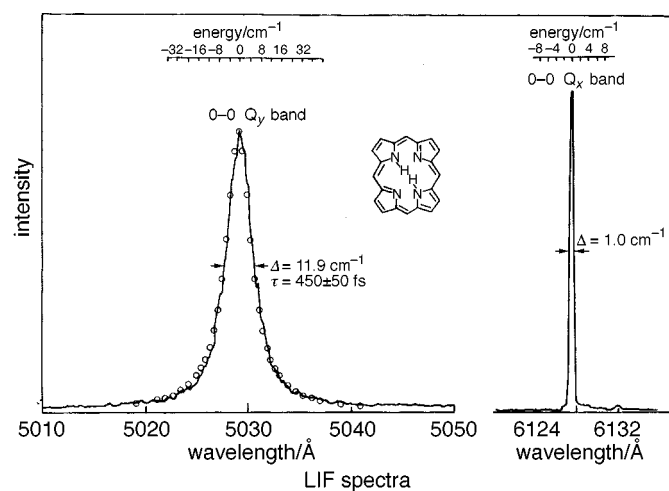


Fig. 5 Absorption of the 0-0 electronic origins of the $S_0 \rightarrow S_2$ (Q_y band) of isolated jet-cooled free base porphyrin. The linewidth ($\Delta = 1.0$ cm^{-1}) of the S_1 origin originated from rotational structure, while the Lorentzian line broadening (fitted by open circles) of the S_2 origin originates from intramolecular coupling and statistical limit $S_2(0-0) \rightarrow S_1^*$ relaxation in a bound level structure (ref. 48).

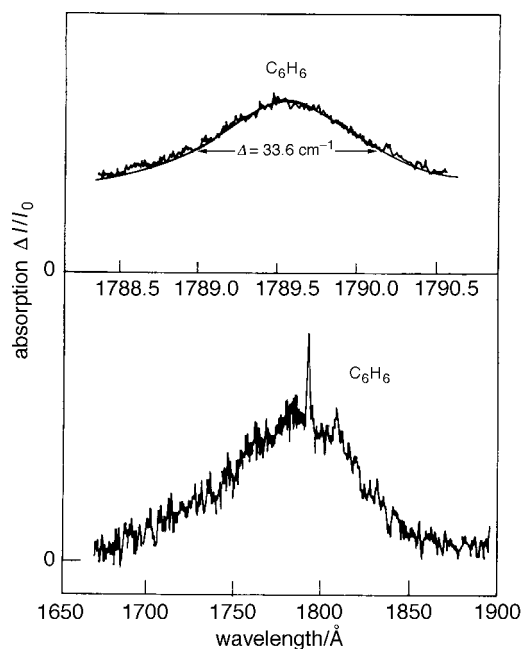


Fig. 6 Absorption spectrum of isolated jet-cooled benzene. Note the sharp feature, which corresponds to the $n = 3$ Rydberg. The upper panel shows the lineshape analysis of the Ru ($3R_u$) Rydberg, which is Lorentzian (fitted by a solid line) with a lifetime of $\tau = 154$ fs for C_6H_6 (and $\tau = 188$ fs for C_6D_6), exhibiting a small deuterium effect. Note that the Rydberg relaxation is considerably slower than the intravalence $\pi\pi^*$ excitation in the same energy domain (ref. 24 and 51). Also note the lack of resonance Rydberg- $\pi\pi^*$ background interference effects (ref. 51).

Table 1 Electronic relaxation lifetimes in isolated jet-cooled molecules^a

molecule	channels	τ /fs	footnotes
azulene S_1	$S_1 \rightarrow S_0$ $\Delta E = 14400 \text{ cm}^{-1}$	800 ± 200	<i>b, c</i>
phenanthrene S_2	$S_2 \rightarrow S_1$ $\Delta E = 4684 \text{ cm}^{-1}$	500 ± 100	<i>b, c</i>
free-base porphyrin $S_2(Q_y)$	$S_2 \rightarrow S_1$ $\Delta E = 3540 \text{ cm}^{-1}$	450 ± 50	<i>b, c</i>
Zn-tetraphenyl porphyrin	$S_2 \rightarrow S_1$	3200 ± 300	<i>b, c</i>
benzene (H_6)	$3nRy \rightarrow \{S_n\} \rightarrow S_0$	160	<i>b, c</i>
benzene (D_6)		190	
$n = 3$ Rydberg			
benzene $S_3(^1E_{1u})$	$S_3 \rightarrow \{S_n\} \rightarrow S_0$	(20)	<i>b, d</i>
benzene $S_2(^1B_{1u})$	$S_2 \rightarrow S_1 S_0$	40	<i>d, e</i>
anthracene $n = 3$ Rydberg	$3nRy \rightarrow \{S_n\} \rightarrow S_1 \rightarrow S_0$	180	<i>b, c</i>
anthracene $S_3(^1B_{3u}^+)$	$S_3 \rightarrow S_1 \rightarrow S_0$	(7)	<i>b, c</i>
fluoranthene S_4	$S_4 \rightarrow S_3 \rightarrow$	60	<i>b, f</i>
1,2-benzanthracene S_3	$S_3 \rightarrow S_2 \rightarrow$	136	<i>b, g</i>

^a Electronic origin of electronic transition. ^b From Lorentzian line broadening. ^c Tel Aviv work (ref. 47–51). ^d Lifetime data. ^e Ref. 52a. ^f Ref. 52b. ^g Ref. 52c.

B Mode selectivity

Current experimental and theoretical progress allows for the control of intramolecular and intermolecular dynamics *via* passive control of energy acquisition when the system evolves under its own Hamiltonian, as well as by active control of energy storage and disposal by the modification of the equations of motion by an external laser field.⁵⁵ The characteristics of interstate coupling and intramolecular relaxation in a large isolated molecule can be more complex and interesting due to resonance effects, providing means for mode-selective dynamics.^{56,57} Mediated intersystem crossing from an S_1 vibronic state to the dense lowest triplet $\{T_1\}$ manifold can be induced by the sequential coupling *via* a sparse manifold $\{T_x\}$ of vibronic states corresponding to a higher triplet state. The theory of mediated $S_1 \xrightarrow{V_{so}} \{T_x^k\} \xrightarrow{V_{vib}} \{T_1\}$ coupling and relaxation^{29,56,57} predicts the occurrence of resonances originating from $\{T_x\} - \{T_1\}$ vibronic coupling (V_{vib}), which mediate the decay of the S_1 doorway state induced by spin-orbit (V_{so}) coupling. Dramatic vibrational mode-selective effects are revealed in the absolute fluorescence quantum yields from photoselected vibronic levels in the S_1 manifold of 9,10-dibromoanthracene^{56,57} (Fig. 7), where the irregular variance of the nonradiative lifetimes spans about three orders of magnitude. These resonance effects for the decay of the S_1 state span the excess vibrational energy range $E_{vib} = 0 - 800 \text{ cm}^{-1}$ above the electronic origin of the S_1 electronic manifold, while at higher E_{vib} mode selectivity is eroded due to intramolecular vibrational energy distribution.

C Towards chemistry. Long-range electron transfer in isolated supermolecules

Electron transfer (ET) reactions in chemistry, physics and biology have been almost exclusively explored in donor (D)–acceptor (A) systems embedded in a medium, *e.g.*, solvent, glass or protein. The seminal Marcus theory of ET^{9,58} encompasses a broad spectrum of systems, *e.g.*, ion in solution, supermolecules and biomolecules, with the solvent coupling playing a central role in dynamics. Intramolecular ET can be realised as an interstate radiationless transition, with the vibronic quasicontinuum acting as a dissipative channel.^{59–62} We have challenged the conventional wisdom regarding the dominating role of medium coupling in ET, proposed long-range ET which occurs in an isolated solvent-free supermolecule DBA (where B is a molecular bridge), and analyzed

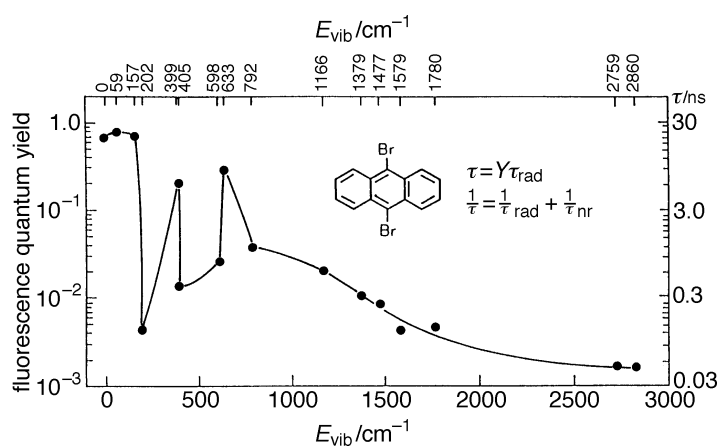


Fig. 7 Absolute fluorescence quantum yields (Y) and lifetimes (τ) of the photoselected vibronic level of jet-cooled 9,10-dibromoanthracene, which exhibit a marked mode selectivity in the vibrational energy range $0 \leq E_{vib} \leq 800 \text{ cm}^{-1}$ above the electronic origin (ref. 63)

the structural and energetic constraints for the occurrence of this radiationless transition.^{59,60} The order of the singlet electronic states of an isolated supermolecule exhibiting ET should involve the ground state $S_0(\text{DBA})$, the charge transfer state $S_1(\text{D}^+\text{BA}^-)$ and the localized excitation $S_2(\text{DBA}^*)$. A single vibronic level of $S_2(\text{DBA}^*)$ can act as a doorway state for internal conversion to the $S_1(\text{D}^+\text{BA}^-)$ quasicontinuum. The ladder diagrams for intramolecular ET are isomorphous to Fig. 1 and 2. It is gratifying that resonance Raman⁶³ and optical lineshape data⁶⁴ will allow for the quantification of these ladder diagrams. The realization of the molecular limit for ET^{59,60} in a (neutral) DBA requires an appropriate electronic level structure, being subjected to the structural–energetic constraints for the D–A (center-to-center) distance^{65,66} $R_{\text{DA}} \leq e^2/[I(\text{D}) - E(\text{A}) - E_{00}]$, i.e., $R_{\text{DA}} \leq 7\text{Å}$, where $I(\text{D})$, $E(\text{A})$ and E_{00} denote the ionization potential of D, the electron affinity of A and the electronic origin of the $(\text{DBA})^*$ transition. For small polaron transfer in D^-BA and hole transfer in D^+BA there are no constraints on R_{DA} .⁵⁹ The prediction for structural constraint in DBA was borne out by Wegewijs and Verhoeven⁶⁵ for ET in isolated jet-cooled rigid supermolecules, with D = dimethoxynaphthalene, A = dicarboxymethoxy ethylene or dicyanoethylene and B = norbornyl-like bridge with N bonds (denoted as DB_NA). $S_2(\text{DBA}^*) \rightarrow S_1(\text{D}^+\text{BA}^-)$ ET was observed for $N = 3$ with $R_{\text{DA}} = 5.8 \text{Å}$, as expected. The theory provides dynamic rules for ET in isolated supermolecules. The theory⁵⁹ also predicts the formation of giant D^+BA^- dipoles, with dipole moment $\leq 35 \text{D}^\dagger$ in molecular beams. Microscopic (state-selective) ET rates are given in the statistical limit in the form^{59–62} $k_s = (2\pi/\hbar)V^2\text{AFD}(E_s)$ in terms of a product of an electronic coupling (V) and the nuclear Franck–Condon overlap density $\text{AFD}(E_s)$. Isolated molecule ET rates exhibit the energy gap (ΔE) dependence (Fig. 8), with typical ET rates in the range $k_s = 10^7\text{--}3 \times 10^8 (V/\text{cm}^{-1})^2 \text{s}^{-1}$ for charge separation from the electronic origin of the $S_2(\text{DBA}^*)$ state. For the DB_NA molecules ($N = 3$) $k_s \geq 10^{14} \text{s}^{-1}$ (ref. 65) in accord with our estimate with $V \approx 1000 \text{cm}^{-1}$. Another, more complex and interesting, isolated-molecule ET pertains to the DBA molecule with D = aniline and A = cyanonaphthalene, held together by a semirigid bridge⁶⁰ (Fig. 9). Long-range ET in the extended structure, followed by

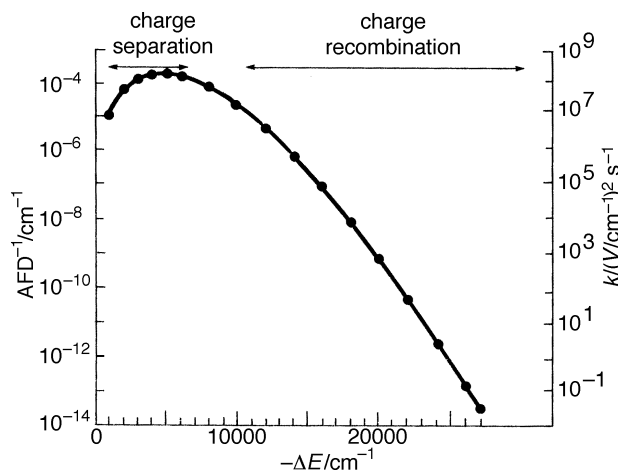


Fig. 8 ET dynamics in isolated supermolecules. The energy gap ($-\Delta E$) dependence of the averaged Franck–Condon density (AFD) and the rate $k = (2\pi/\hbar)V^2\text{AFD}$ for the electronic origin. Calculations for a four intramolecular vibrational level system (ω/cm^{-1}) = (200, 500, 1200, 1500) with couplings $S = (6, 3, 1, 1)$. Note the exponential energy gap for charge separation at large $-\Delta E$ (ref. 99).

\dagger 1 D (debye) $\approx 3.33564 \times 10^{-30} \text{C m}$.

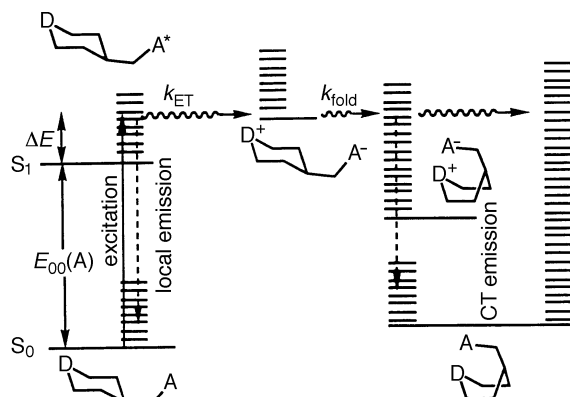


Fig. 9 Sequential long-range electron transfer and electrostatically driven conformational folding in an isolated semirigid DBA molecule. Isolated-molecule ET dynamics is described by a mediated intramolecular radiationless transition (ref. 60).

electrostatically driven conformational folding (Fig. 9),^{66,67} was described⁶⁰ in terms of mediated nonradiative ET. This analysis builds a bridge between ET and intramolecular radiationless transitions. Unifying features of intramolecular dynamics can be applied to predict and describe other nonadiabatic processes, *e.g.*, electronic energy transfer and spin-conversion in isolated supermolecules, opening up new areas of intramolecular chemistry.

D Electronic quasicontinuum

Up to this point we were concerned with intramolecular dynamics within a vibrational quasicontinuum, manifesting nuclear motion. Very high n (equal to 50–250, where n is the principal quantum number) molecular Rydberg states are characterized by a high density ($\rho \propto n^3/\text{Ry}$, where Ry is the Rydberg constant) of electronic states and by unique intramolecular $nl-n'l'$ coupling which involves core–multipole interactions in the absence of an external (weak) electric field.^{70–72} A generalization and unification of the theory of intramolecular coupling and dynamics for a Rydberg manifold was provided, establishing the conditions for strong coupling of a doorway Rydberg state and the attainment of the statistical limit within an electronic quasicontinuum.⁷² Another interesting aspect of the dynamics of a Rydberg manifold pertains to the preparation and interrogation of a wavepacket of electronic states.⁷²

Correlations in continua and quasicontinua determining dynamics on the timescale of nuclear motion

Radiationless processes in molecular and cluster systems involve the following decay channels (Fig. 10).

- (1) ‘Reactive’ nonradiative channels for molecular (rotational, vibrational or electronic) autoionization or predissociation.
- (2) ‘Nonreactive’ channel for electronic–vibrational relaxation or IVR within a bound level structure involving the vibronic quasicontinuum.
- (3) The electronic quasicontinuum of an ultrahigh Rydberg manifold.

The dissipative channels for intramolecular dynamics can be characterized in terms of the state specificity of the matrix elements of the Hamiltonian (H), *i.e.*, $V_{s1} = \langle s | H | 1 \rangle$, for the coupling of the doorway states $|s\rangle$, $|s'\rangle$, $|s''\rangle$... with the $\{|1\rangle\}$ states of the continuum or quasicontinuum. The state dependence of the couplings is quantified by

Intramolecular dynamics
Isolated molecules

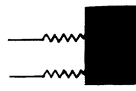
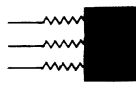
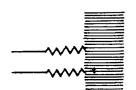
relaxation process	dissipative channel
autoionization (1930–)	ionization continuum 'smooth' coupling 
predissociation (1928–)	dissociation continuum 'smooth' coupling 
radiationless transitions bound level structure (1968–)	vibronic Franck–Condon quasicontinuum 'bumpy' weakly correlated coupling 
electronic relaxation ultrahigh Rydbergs (1996–)	electronic quasicontinuum 'smooth' coupling 

Fig. 10 Intramolecular dynamics in isolated molecules

the correlation parameter^{68,69,73}

$$\eta_{ss'} = \langle V_{s1} V_{s'1} \rangle / [\langle V_{s1}^2 \rangle \langle V_{s'1}^2 \rangle]^{1/2} \quad (5)$$

where $\langle \rangle$ denotes average products over the energy range which includes E_s and $E_{s'}$. The continua and quasicontinua can be segregated into: (i) 'smooth' decay channels, involving slow energy dependence (E_1) of V_{s1} , with $\eta_{ss'} = 1$ for $s \neq s'$, *i.e.*, dissociative and ionizative continua and the electronic quasicontinuum, and (ii) 'nonsmooth' decay channels, where V_{s1} exhibits a large and irregular energy (E_1) variation, $\eta_{ss'} \ll 1$, where $s \neq s'$, *i.e.*, the vibrational Franck–Condon quasicontinuum. The distinction between 'smooth' and 'nonsmooth' channels does not affect the level structure and dynamics of molecular eigenstates which have their parentage in a single doorway state coupled to a single quasicontinuum. This distinction is of central importance for interference effects between several doorway states, which exhibit a profound influence on femtosecond intramolecular dynamics in electronically–vibrationally excited wavepackets of states of large isolated molecules and in the condensed phase. The correlation parameters $\eta_{ss'}$ determine vibrational coherence in nonradiative dynamics⁷³ and determine the upper temporal limits for relaxation.⁶⁹

For intramolecular relaxation processes involving a 'smooth' correlated ($\eta_{ss'} \approx 1$), dissipative channel, the temporal constraints on the dynamics can be inferred from the theory of overlapping resonances^{74,75} which sets an upper limit on k . For the population of a set of equally spaced (nearest neighbor separation of ω) resonances (of widths $\Gamma = 2\pi V^2 \rho$ for an isolated resonance), interference effects set in when $\Gamma \approx \omega$. The intramolecular relaxation rate is $k = (\Gamma/\hbar) / [1 + (\pi\Gamma/\omega)]$. The rate exhibits a transition from $k = (\Gamma/\hbar)$ for an isolated resonance ($\Gamma \ll \omega$) to $k = \omega/h$ for overlapping resonances

($\Gamma \gg \omega$). The overlapping resonance domain provides an upper limit for the nonradiative rates, *i.e.*, $k \leq \omega/h$, which is determined by the level spacing, *i.e.*, the vibrational frequency (timescale $t \approx k^{-1} \approx 10\text{--}1000$ fs). This situation prevails for intramolecular dynamics in a ‘smooth’ nuclear continuum, *i.e.*, electronic and vibrational predissociation. The experimental ultrafast fs electronic predissociation times of diatomics⁷⁶ are limited by the overlapping resonances constraint. For dynamics in the ‘smooth’ electronic Rydberg quasicontinuum the upper limit for the rate is $k \leq 2Ry/n^3\hbar$ (*i.e.*, k for $n = 50$ being in the ps^{-1} domain).

For the decay of weakly correlated ($\eta_{ss'} \ll 1$) overlapping resonances into a ‘nonsmooth’ Franck–Condon vibrational quasicontinuum, interference effects are expected to be much less pronounced than for the case of a ‘smooth’ channel. This is experimentally manifested in the related context of the lack of interference effects, *i.e.*, Fano antiresonances in the absorption spectra of Rydberg states which overlap $\pi\pi^*$ intravalence excitations in large aromatic molecules (Fig. 6). Model calculations of correlation parameters $\eta_{ss'}$ for a doorway state in the vicinity of the electronic origin are considerably lower than unity, with their highest values falling in the range $|\eta_{ss'}| = 0.4\text{--}0.2$ for a small number of s, s' pairs differing only by a single vibrational quantum number, while for multimode s, s' changes very low values of $|\eta_{ss'}| < 0.1$ are exhibited.^{68,69,73} These propensity rules imply the existence of weak correlations within the Franck–Condon vibrational quasicontinuum, resulting in a partial erosion of resonance interference effects, in some analogy with random coupling models for intramolecular coupling and dynamics,^{76–78} where interference effects are completely eroded. Ultrafast intramolecular radiationless transition rates in a bound level structure of overlapping resonances into the Franck–Condon quasicontinuum are expected not to be strictly limited by the level spacing, but rather the temporal upper limit $k \propto V^2 \geq \omega/h$ can be realized. Indeed, some of the ultrafast (*ca.* 10 fs) relaxation times of intravalence excitations of isolated aromatic molecules (Table 1) exceed most of the intramolecular frequencies. Such temporal records may be achieved for ‘nonreactive’ radiationless transition in large molecules and for nonadiabatic processes in liquids, solids and proteins, providing a unification of intramolecular and condensed phase ultrafast dynamics.

Perspectives for future studies of ultrafast dynamics in large isolated molecules pertain to the following.

(1) High-energy intravalence and Rydberg excitations of large molecules will constitute a hunting ground for fs intramolecular time-resolved dynamics in electronic origins of jet-cooled isolated molecules (Table 1). These data, which approach or exceed the timescale for intramolecular frequencies, are important in the context of intramolecular dynamics in the Franck–Condon quasicontinuum. Temporal records on the timescale for ultrafast interstate dynamics will prevail.

(2) Time-resolved chemistry in isolated supermolecules and linomolecules, mode selectivity and coherent single molecule chemistry. Some of the interesting problems involve electrons in a single supermolecule resulting in the formation of a giant dipole, hole transfer in an isolated polypeptide, with the possible distinction between transfer and transport, vibrational coherence in intramolecular chemistry, vibrational mode selectivity in ET and in EET, and coherent *vs.* incoherent electronic energy transfer.

(3) Quantum beats. The time evolution of a coherently excited wavepacket of molecular eigenstates will exhibit interference effects. For large molecules such wavepackets can manifest (i) molecular eigenstates originating from interstate or intrastate coupling; (ii) Jahn–Teller coupled vibronic manifold in doubly degenerate states of a large molecule, *e.g.*, the E state of triptycene, which bears analogy to the adiabatic–diabatic coupling in IBr studied by Stollow;⁷⁹ (iii) electron–vibrational coherence in mediated coupling; (iv) electron–vibrational coherence in intramolecular chemistry.

(4) Dynamics of ultrahigh n ($=50\text{--}250$) molecular Rydbergs. Timescales for the longevity of molecular Rydberg states in I_2 were explored by Stollow⁷⁹ by nuclear

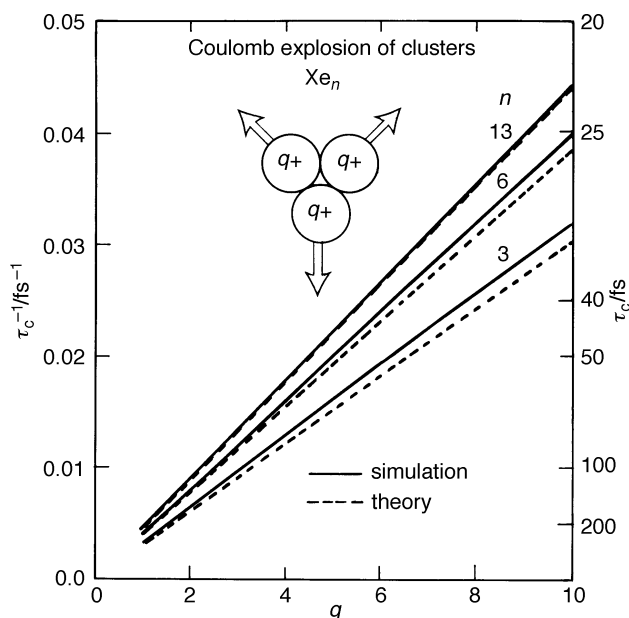


Fig. 11 Coulomb explosion dynamics of $(\text{Xe}^{q+})_n$ clusters. The ion charge is $q = 1-10$ (ref. 84). The Coulomb explosion times from the classical equation⁸⁴ is in accord with the results of molecular dynamics simulations. Note the $\tau_c^{-1} \propto q$ dependence, in accord with the classical picture.

wavepacket dynamics. Of considerable interest is the coherent excitation and interrogation of an electronic wavepacket of high n molecular Rydbergs. An interesting related problem involves the dynamics of a wavepacket of one-dimensional Rydberg states of an excess electron bound to a metal or dielectric surface by image forces.⁸⁰

Dissociative dynamics and Coulomb explosion in molecules and clusters

For direct dissociation in molecular systems the dynamics involves the sliding on a repulsive potential surface.⁸ The characteristic time for dissociation is described in terms of the classical mechanical model of Zewail and co-workers^{81,82} $\tau_c = \int_{R_0}^R dR'/v(R')$, where $v(R')$ is the velocity at R' . This simple description captures the essential features of the dynamics. The typical timescale for direct dissociation is $\tau_c \approx 100$ fs.

An ultrafast excitation leading to the localization of energy in polyatomic molecules or clusters can be achieved by a Coulomb explosion.^{83,84} This ultrafast process is characterized by site selective energy acquisition in conjunction with bond-specific energy disposal. The mechanical model for the separation of two positive ions of charges q_1 and q_2 with an effective mass (μ/AM where $AM = \text{atomic mass}$) initially separated at distance ($R_0/\text{\AA}$) to the distance ($R/\text{\AA}$), gives⁸⁴ $(\tau_c/\text{fs}) = 1.9R_0(\mu R_0/q_1 q_2)^{1/2}Z(\xi)$, where $\xi = R_0/R < 1$ and the numerical function $Z(\xi) \approx 1$ for $\xi = 1/2$. The timescales for Coulomb explosion reflect fs dynamics being shorter by about 1–2 orders of magnitude than the corresponding timescales for molecular dissociation. The timescales obtained from the classical model for the explosion of an $(\text{Xe}^{+q})_n$ cluster reveal that $\tau_c^{-1} \propto q$, being borne out by molecular dynamics simulations (Fig. 11). The utilization of the ultrafast fs ‘chemical clock’ of Coulomb explosion of molecules,⁸³ surface states,⁸³ and clusters^{84,85} precludes IVR and shows potential applications for selective chemistry.

Cluster dynamics

Clusters, *i.e.*, finite aggregates containing $2\text{--}10^9$ constituents, provide novel insight into the dynamics of systems with finite density of states, where separation of timescales can be realized. A key concept for the quantification of the unique characteristics of clusters pertains to cluster size effects.^{40,41,43,86,87} These involve the evolution of structural, thermodynamic, electronic, energetic, electrodynamic and dynamic features of finite systems with increasing cluster size. Several interesting dynamic cluster size effects were explored theoretically by modeling and by simulations.

(1) The ‘transition’ from molecular-type dissociative dynamics in small clusters to condensed-matter type nonreactive vibrational relaxation in large clusters manifests the bridging between molecular and condensed phase nuclear dynamics.^{43,86,87}

(2) Collective vibrational modes.^{87,88} Interior, collective, compression nuclear modes of molecular clusters (He_n , Ar_n) can be treated in terms of the excitation of a liquid drop and were experimentally documented. Complementary to the energetics of these collective modes, their dynamics is interesting. The damping of the collective motion *via* the coupling of a ‘giant resonance’ to non-coherent vibrational modes, constitutes a theoretical and experimental challenge.

(3) Bubble dynamics. The dynamics of large local configurational charge are induced by an extravalence excitation of a probe atom (*e.g.*, $^1\text{S}_0 \rightarrow ^3\text{P}_1$ excitation of Xe) or molecule (*e.g.*, Rydberg excitation of NO) in a rare-gas cluster.⁸⁹ Molecular dynamics simulations of the dynamics of configurational nuclear relaxation around the $^3\text{P}_1$ excitation of Xe in XeAr_n clusters (Fig. 12) reveal: (i) large configurational dilation, *i.e.*, ‘bubble’ formation on the timescale of $t_B \approx 100\text{--}300$ fs; (ii) t_B marking the timescale for ultrafast energy transfer; (iii) multimodal time evolution, with slower timescales of 1–5 ps; (iv) marked impact vibrational coherence excitation (this vibrational coherence characterizes the collective vibrations around the excited probe atom with a long timescale for dephasing of 1–5 ps, considerably exceeding the timescale for initial configurational relaxation).

(4) Ultrafast energy acquisition *via* high-energy cluster–wall collisions.⁹⁰ High-energy impact of atomic or molecular cluster ions (of sizes 10–1000 constituents, with

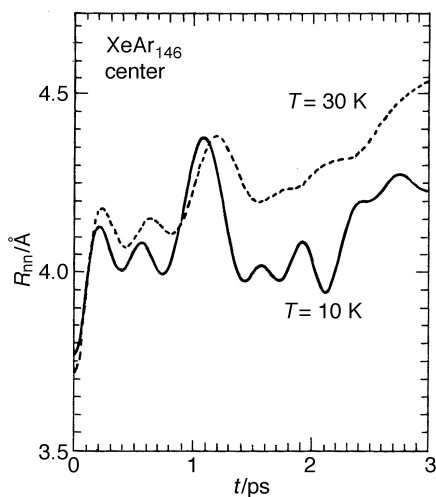


Fig. 12 The time evolution of the average Xe–Ar distance R_{nn} of $\text{Xe}(^3\text{P}_1)$ at the central site in XeAr_{146} . $T = 10, 30$ K mark the equilibrium cluster temperature prior to excitation. Configurational dilation is manifested by the increase of R_{nn} on the timescale of *ca.* 200 fs. Note the impact vibrational coherence by oscillations in R_{nn} .

velocities up to $v \approx 20 \text{ km s}^{-1}$ and kinetic energies up to *ca.* 100 eV per particle) on insulator, semiconductor or metal surfaces, produces a new medium of extremely high density (up to *ca.* 2–4 times the standard density), high temperature (up to *ca.* 10^5 K) and high energy density (up to 10^2 eV per particle), which is temporarily generated during the propagation of a microshock wave within the cluster on the 10^2 – 10^3 fs time-scale. Chemical applications, *e.g.*, cluster impact dissociation of a probe diatomic molecule (Fig. 13), were attempted. The dissociation process is limited by the vibrational period of the molecule.

Perspectives of future explorations of cluster dynamic size effects pertain to the following.

(1) Real-time probing of adiabatic nuclear motion on multidimensional potential surfaces. These will involve preparation, *e.g.*, (passive) vibrational mode selectivity and

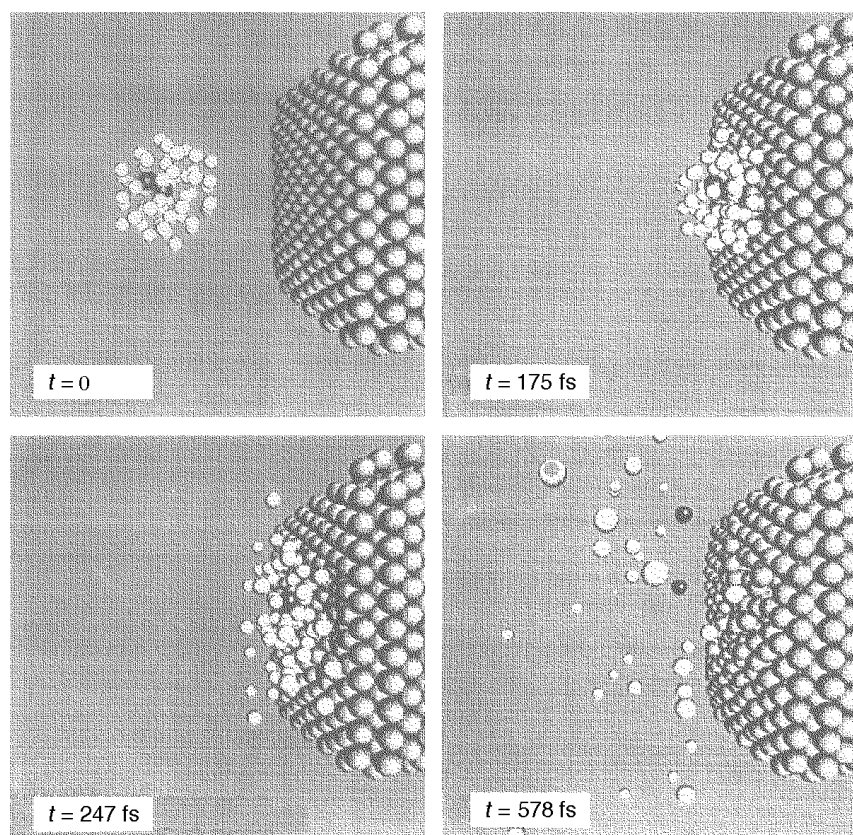


Fig. 13 Snapshots of molecular dynamics simulations of the collision of an I_2Ar_{53} cluster with a Pt surface. The guest I_2 molecule (black balls) is located in an interior state within the Ar cluster (white balls). The Pt surface (grey spheres) consists of six layers of 120 atoms each. The cluster temperature is 10 K and the surface temperature is 300 K. The times are marked on the four snapshots. At $t = 0$, the cluster with the initial center of mass velocity of $v = 10 \text{ km s}^{-1}$ ($E_k^0 = 1.23 \times 10^3 \text{ eV}$) is located at a center of mass distance of 20 \AA from the wall. At $t = 175 \text{ fs}$, the cluster–wall impact achieves a peak of the cluster potential energy. Subsequently, cluster fragmentation occurs at $t = 247 \text{ fs}$, while at $t = 578 \text{ fs}$, the dissociation of I_2 is clearly exhibited (ref. 90). For $E_k^0/N = 10$ – 30 eV the average dissociation time for I_2 falls in the range $\langle \tau_D \rangle = 200$ – 150 fs , which is comparable to, or shorter than, the vibrational time $\tau_v = 156 \text{ fs}$ of the guest I_2 molecule. This process manifests thermal fs dynamics on the timescale of nuclear motion.

energy storage, *e.g.*, intracluster vibrational energy redistribution. This problem is also central in biophysics, pertaining to protein folding.^{90,91}

(2) Real-time dynamics of nuclear configurational changes. The real-time interrogation of cluster isomerization and of rigid–nonrigid transformation (*i.e.*, ‘melting’) will be of considerable interest.

(3) Impact-induced vibrational coherence. These are induced by short-range repulsive interactions with intracluster dissociation fragments in I_2Ar_n (ref. 92) or $I_2^-Ar_n$ (ref. 94) or by Rydberg excitation, *e.g.*, Xe^*Ar_n ,⁸⁹ and manifest the excitation of a vibrational wavepacket.

(4) Interstate fs dynamics in clusters. Radiationless electronic–vibrational relaxation in metal_n clusters will elucidate the interrelations between electronic level structure and dynamics.

(5) Temporal records for nuclear dynamics. These include the Coulomb explosion of highly charged clusters.^{84,85}

(6) Real-time dynamics of elementary excitations in finite systems. These will involve collective compression nuclear modes and phonons. More esoteric elementary excitations constitute rotons (vortex rings) in quantum boson systems, *e.g.*, $(^4He)_n$ with $n > 100$ or possibly $(H_2)_n$, which can be studied by two-particle excitations in the electronic origin of a probe molecule in the cluster.⁹⁵

(7) Thermal fs chemistry. Cluster impact dynamics *via* high-energy cluster–wall collisions or cluster–cluster collisions open up a new research area of thermal femtosecond chemistry.

Condensed phase dynamics

The pioneering studies of Kubo^{6,8} on electron–hole recombination in semiconductors, of Marcus on ET in solution⁹ and of Förster on EET in the condensed phase,¹⁰ laid the foundations for the theory of nonadiabatic dynamics in the condensed phase and in protein medium. The isomorphism between condensed phase nonadiabatic dynamics and intramolecular radiationless transitions was addressed⁹⁶ in the context of the incorporation of quantum effects in ET theory. Both condensed phase and intramolecular radiationless transitions are induced by the coupling of doorway state(s) to a vibronic quasicontinuum. A unified conceptual framework for all these condensed phase radiationless transitions considers population relaxation between two potential surfaces of the entire system corresponding to distinct zero-order electronic configurations with energy conservation being insured by absorption and emission of medium phonons and intramolecular vibrations. For a nonradiative process from a reactant doorway vibronic state $|s\rangle$ to the vibronic manifold $\{|\alpha\rangle\}$ of product states quasidegenerate with it, which is induced by the electronic couplings V , the microscopic rate is given by the golden rule expression

$$k_s = (2\pi/\hbar) |V|^2 F_s \quad (6)$$

where the Franck–Condon densities are

$$F_s = \sum_{\alpha} |\langle s|\alpha\rangle|^2 \delta(E_s - E_{\alpha}) \quad (7)$$

We proceed to consider the broad field of ET. A basic assumption underlying the microscopic description of the rate k of such nonadiabatic processes in terms of the microscopic rates (6) is the insensitivity of the ET dynamics to the medium dynamics, which can be realized under one of the following conditions. (i) The common situation of fast medium vibrational dynamics, which allows the separation of timescales between

the fast medium relaxation and slow ET, with the microscopic ET rate constants constituting the rate determining step. Under these circumstances the finite temperature rate k is expressed^{96,97} in terms of a thermal average $k = \sum_s P_s k_s$, where P_s is the thermal population of level $|s\rangle$. (ii) The microscopic rates depend weakly on the initial vibronic manifold. Under these circumstances $k \approx k_s$ (for the relevant doorway states). Such a state of affairs prevails for activationless ET, where the potential surfaces cross in the vicinity of the minimum of the initial state, which pertains to the optimization of the ET rate. Weak state specific k_s also prevails for inverted region ET where high frequency vibrations of the D and A centers result in intramolecular vibrational excitation induced by ET.⁹⁷

Ultrafast femtosecond ET reactions in condensed phase are expected to correspond to activationless ET. Such reactions are not limited by solvent dynamics,^{98,99} which was traditionally specified by the solvent relaxation time $\langle\tau\rangle$ induced by a constant charge, with the solvent adiabaticity parameters $\kappa = 4\pi|V|^2\langle\tau\rangle/\hbar\lambda$. For $\kappa \gg 1$ an activationless ET would apparently be characterized by $k \approx \langle\tau\rangle^{-1}$, setting an upper limit on the rate. This expectation was violated^{98,99} by several ET experiments with ET rates in the range $(80\text{--}1000)^{-1} \text{ fs}^{-1}$, which resulted in $k\langle\tau\rangle = 50\text{--}100$. The origin of the failure of the theory of solvent controlled ET was traced to the weak excess energy dependence of the microscopic rates^{98,99} for the activationless (and the inverted region) process, which implies that ET cannot be described by diffusion towards the intersection of the potential energy surfaces at the minimum of the initial DA surface. Rather, the depletion dynamics of the DA manifold occurs from an entire manifold of doorway states. ET fs dynamics is limited by the electronic coupling and the nuclear Franck–Condon factors, in analogy to intramolecular dynamics. Perspectives of future studies of condensed phase dynamics pertain to the following.

(1) Real-time dynamics of elementary excitations, *e.g.*, excitons, phonons, vibrons or rotons, in the context of one-particle and two-particle excitations.

(2) Real-time dynamics of configurational relaxation induced by electron solvation in fluids. The interesting adiabatic electron bubble formation equilibrium radius 17 Å at zero pressure in liquid He, Ne or H₂ was studied theoretically,^{100,101} considering a combination of quantum mechanical and hydrodynamic effects, and should be subjected to experimental scrutiny.

(3) Dynamics of medium structure. The exploration of the time dependent correlation function $g(r, t)$, following the excitation of a probe ion or molecule in a fluid conducted by Hochstrasser,¹⁰² is novel and interesting.

(4) Interstate energy and phase relaxation in the Franck–Condon vibronic quasicontinuum. Nonadiabatic fs dynamics is governed by electronic coupling (V) and nuclear Franck–Condon factors. The coupling to the vibronic quasicontinuum is weakly correlated (*i.e.*, small $\eta_{ss'} < 0.3$ for multimode model systems) resulting in high rates ($\propto V^2$) and in phase erosion.^{71–73} Further exploration of ultrafast fs EET and ET processes^{102–106} will be of interest.

(5) Temporal records on rates for nonadiabatic dynamics. Recent experimental studies on ET dynamics¹⁰⁵ established timescales of 80–100 fs, while studies of EET between prosthetic groups in the photosynthetic reaction center and EET in photosynthetic antennas^{103,104,106} established timescales of 50–100 fs. These ultrafast timescales for ET and EET ($\tau = 50\text{--}100$ fs) correspond to vibrational frequencies of $(c\tau)^{-1} \approx 300\text{--}600 \text{ cm}^{-1}$, *i.e.*, being on the timescale of the intramolecular frequencies and considerably exceeding the frequencies of medium (or protein) modes. The theory of radiationless transitions in the (weakly correlated) Franck–Condon quasicontinuum indeed predicts that the characteristic times can exceed the vibrational period.^{71–73}

(6) The ubiquity of vibrational coherence effects ranging from small to huge systems^{102–104,107} raises the conceptual question of the distinction between the experimental condition of the preparation and interrogation on one hand, and the intrinsic

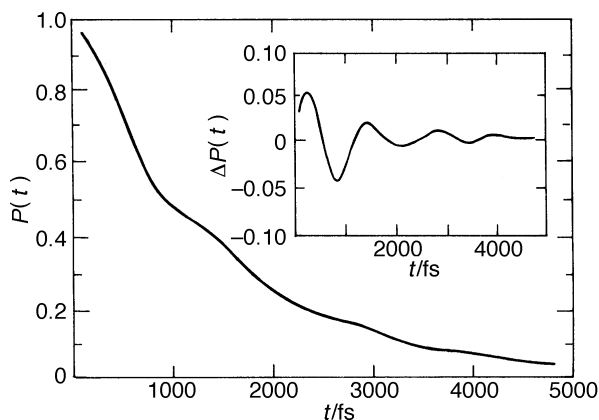


Fig. 14 Temporal vibrational coherence in nonadiabatic dynamics, showing the nonradiative decay probability $P(t)$ of the reactants manifold to a vibronic quasicontinuum. Data for a four-mode Franck–Condon system with frequencies $\omega/\text{cm}^{-1} = (117, 75, 35, 27)$, coupling parameters $S = (1.0, 1.1, 1.2, 3.0)$, energy gap $\Delta E = 500 \text{ cm}^{-1}$ and electronic coupling $V = 20 \text{ cm}^{-1}$. The initial wavepacket consists of the seven lowest states in the doorway manifold with the amplitudes given by the appropriate vibrational overlap integrals from the ground electronic–vibrational state. The inset shows the time dependence of $\Delta P(t) = P(t) - A_v[P(t)]$, reflecting low amplitudes of the quantum beats.

aspects of relaxation and dephasing dynamics on the other hand. The manifestation of quantum beats in nonadiabatic dynamics (Fig. 14) is determined by:⁷¹ (i) spectroscopic information, *i.e.*, transition moments and periods, and (ii) dynamic information, *i.e.*, modulation amplitudes and (low) correlation parameters $\eta_{ss'}$. For the excited state population probability, weak modulation reflects dynamics information, while the quantum beats in the photon counting rates from the bacteriochlorophyll dimer in the photosynthetic bacterial reaction center just provide spectroscopic information.

(7) Homogeneous *vs.* heterogeneous broadening. These pertain to spatial effects, *e.g.*, diagonal Anderson-type and off-diagonal disorder which result in localization,¹⁰⁸ and to temporal effects, which are reflected in the spectral density.¹⁰⁶

Some facets of biophysical dynamics

Remarkable progress has been made in biophysical ultrafast dynamics, with the experimental and the theoretical microscopic exploration of the primary processes of EET in photosynthetic antennae¹⁰⁴ and ET in photosynthetic reaction centers.¹⁰⁹ The ultrafast EET processes (timescales from *ca.* 100 fs to ps) in different (nonuniversal) antenna structures effectively preclude energy waste. The basic issues which pertain to the mechanism and unidirectionality of the primary charge separation in the (universal) reaction center (RC) structure of photosynthetic bacteria and photosystem II are not yet fully elucidated. These involve the following.

- (1) Optimization principles for the primary ET process.
- (2) Kinetic redundancy for the primary ET process. This will ensure the stability of the photosynthetic apparatus with respect to mutagenesis, chemical modifications and environmental perturbation.
- (3) Structural redundancy. This is manifested in the unique symmetry breaking, *i.e.*, the unidirectionality of the primary charge separation across the ‘active’ A branch of the

RC.¹¹⁰ ET transfer theory implies that unidirectionality is dominated by cumulative effects, *i.e.*, electronic coupling and energetic modification of the energy gap across the 'inactive' B branch. Breaking of the symmetry breaking, *i.e.*, inducing charge separation across the inactive branch, was accomplished by chemical modification of the energetics, which retards the ET process across the active branch of the RC.¹¹¹

The determination of the structure of the photosynthetic bacterial RC¹¹² constituted a seminal accomplishment. Nevertheless, we should challenge the notion of the structure–function relationship, providing a complete description of the central energy conversion process in photobiology. Structural information alone is not sufficient to understand the function of the RC, which rests on the ingredients of ultrafast dynamics. Dynamic information transcends and complements structural data. We should strive toward the broad unification of structure–dynamics–function relations in ultrafast biophysical and chemical dynamics.

Concluding remarks

We explored the rich and fascinating world of the dynamics of electronically–vibrationally excited states of isolated molecules, clusters, condensed phase and biological systems on the timescale of nuclear motion. Have we reached the temporal borders of the fundamental processes in chemistry and biology? The timescales of intermolecular and intramolecular nuclear motion definitely provide the relevant temporal limit for biological transformations. For chemical transformations even shorter timescales of femtoseconds to attoseconds (*i.e.*, 10–0.1 fs) for electron dynamics will be unveiled. Examples which come to mind in the realm of intramolecular and cluster dynamics involve hole migration in He_n^+ clusters on the 10^{-14} – 10^{-12} s timescale prior to its trapping, as well as early charge delocalization in isolated large molecules, model biomolecules and clusters.¹¹³ In the areas of clusters and condensed phase electron dynamics fascinating processes involve bulk and surface electron–electron collisions and plasmon dynamics, incipient excess electron localization in liquids, electron–hole coherence of Wannier excitons and exciton wavepacket dynamics in semiconductor clusters and quantum dots, dynamics of excess electron external image states on metals and adsorbants on metal surfaces,^{80,114,115} and electron tunneling microscopy in real-time.¹¹⁶ Such chemical transformations involve changes in electronic state(s) without the involvement of nuclear motion, bypassing the constraints imposed by the Franck–Condon principle.

Theory played a central role in establishing the conceptual framework of dynamics in chemistry and biology. From the historical perspective theoretical chemistry, until the 1960s, focused on the nature of the chemical bond. This was beautifully reflected in the address of Charles Coulson at the Boulder Conference on Molecular Structure Calculations in 1959,¹¹⁷ where the goals of theoretical chemistry at that time were defined:

'We may hope that eventually all problems (of molecular structure) in the range of 1–20 electrons will be solved accurately by computational techniques... But surely there is much more in chemistry that covered by this range'.¹¹⁷

Contemporary quantum chemistry has undergone major developments and currently predictions of static molecular structure, molecular properties and intramolecular interactions at the level of chemical accuracy are becoming available. But there is much more in chemistry! The theory of intramolecular, cluster, condensed phase, and biophysical dynamics developed during the last three decades, has been decisive in providing models, insight, information and prediction. Furthermore, without dynamics one cannot understand the function in chemistry and biology. The theory

of chemical and biophysical dynamics on the microscopic level, relating structure, function and dynamics, had an audible impact on the development of modern chemistry.

References

- 1 K. F. Bonhoeffer and L. Farkas, *Z. Phys. Chem. (Leipzig)*, 1928, **134**, 337.
- 2 G. Wenzel, *Z. Phys.*, 1928, **29**, 321.
- 3 H. Eyring and M. Polanyi, *Z. Phys. Chem. Abt. B*, 1931, **12**, 279.
- 4 R. D. Levine and R. B. Bernstein, *Molecular Reaction Dynamics*, Oxford University Press, New York, 1987.
- 5 K. Huang and A. Rhys, *Proc. R. Soc. London A*, 1951, **208**, 352.
- 6 R. Kubo, *Phys. Rev.*, 1952, **86**, 929.
- 7 M. Lax, *J. Chem. Phys.*, 1952, **20**, 1752.
- 8 R. Kubo and Y. Toyozawa, *Prog. Theor. Phys.*, 1955, **13**, 160.
- 9 R. A. Marcus, *J. Chem. Phys.*, 1956, **24**, 966; 979.
- 10 Th. Förster, *Discuss. Faraday Soc.*, 1959, **27**, 7.
- 11 M. Kasha, *Radiat. Res. Suppl.*, 1960, **2**, 243.
- 12 M. Beer and H. C. Longuet-Higgins, *J. Chem. Phys.*, 1955, **23**, 1390.
- 13 G. W. Robinson and R. P. Frosch, *J. Chem. Phys.*, 1962, **37**, 1962.
- 14 M. Gouterman, *J. Chem. Phys.*, 1962, **36**, 2846.
- 15 S. H. Lin, *J. Chem. Phys.*, 1966, **44**, 3759.
- 16 S. H. Lin and R. Bersohn, *J. Chem. Phys.*, 1968, **48**, 2732.
- 17 G. B. Kistiakowski and C. S. Parmenter, *J. Chem. Phys.*, 1965, **42**, 2942.
- 18 M. Bixon and J. Jortner, *J. Chem. Phys.*, 1968, **48**, 715.
- 19 M. Bixon and J. Jortner, *Mol. Cryst.*, 1969, **213**, 237.
- 20 M. Bixon and J. Jortner, *Isr. J. Chem.*, 1969, **7**, 189.
- 21 M. Bixon and J. Jortner, *J. Chem. Phys.*, 1969, **50**, 3284.
- 22 M. Bixon and J. Jortner, *J. Chem. Phys.*, 1969, **50**, 4061.
- 23 J. Jortner, S. A. Rice and R. M. Hochstrasser, in *Advances in Photochemistry*, ed. B. O. Pitts and G. Hammond, Wiley, New York, 1969.
- 24 J. Jortner, *J. Chim. Phys.*, 1970, **9**.
- 25 J. Jortner, *Pure Appl. Chem.*, 1970, **24**, 1675.
- 26 J. Jortner and S. Mukamel, in *MTP International Review of Science*, ed. A. D. Buckingham and C. A. Coulson, Butterworth, London, 1976, vol. 13, p. 327.
- 27 A. Nitzan and J. Jortner, *J. Chem. Phys.*, 1971, **55**, 1355.
- 28 A. Nitzan, J. Jortner and P. M. Rentzepis, *Mol. Phys.*, 1971, **22**, 585.
- 29 A. Nitzan, J. Jortner and P. M. Rentzepis, *Proc. R. Soc. London A*, 1972, **327**, 367.
- 30 A. Nitzan and J. Jortner, *Mol. Phys.*, 1972, **24**, 109.
- 31 A. Nitzan and J. Jortner, *J. Chem. Phys.*, 1972, **57**, 2870.
- 32 B. Berne, A. Nitzan and J. Jortner, *J. Chem. Phys.*, 1974, **61**, 227.
- 33 J. Jortner and S. Mukamel, in *The World of Quantum Chemistry*, ed. R. Daudel and B. Pullman, Reidel, Dordrecht, 1974, 145.
- 34 J. Jortner and S. Mukamel, in *Excited States*, ed. E. C. Lim, Academic Press, New York, 1977, vol. III, p. 57.
- 35 J. Kommandeur and J. Jortner, *Chem. Phys.*, 1978, **28**, 273.
- 36 J. Jortner and R. D. Levine, *Advances in Chemical Physics*, Wiley, New York, 1981, vol. 47, pp. 1–114.
- 37 A. H. Zewail, *Femtochemistry*, World Scientific, Singapore, 1994.
- 38 *Femtochemistry*, ed. M. Chergui, World Scientific, Singapore, 1996.
- 39 *Proceedings of the Nobel Symposium on Femtochemistry and Fentobiology, Ultrafast Reaction Dynamics at Atomic Scale Resolution*, ed. V. Sundström, 1996, in press.
- 40 J. Jortner, ref. 38, p. 15.
- 41 J. Jortner, ref. 39, in press.
- 42 J. Manz, ref. 39, in press.
- 43 J. Jortner, *Z. Phys. D: At. Mol. Clusters*, 1992, **24**, 247.
- 44 S. Mukamel, *Principles of Nonlinear Optical Spectroscopy*, Oxford University Press, Oxford, 1995.
- 45 M. Bixon, Y. Dothan and J. Jortner, *Mol. Phys.*, 1969, **17**, 109.
- 46 J. Jortner and R. S. Berry, *J. Chem. Phys.*, 1968, **48**, 2757.
- 47 A. Amirav and J. Jortner, *J. Chem. Phys.*, 1984, **81**, 4200.
- 48 U. Even and J. Jortner, *J. Chem. Phys.*, 1982, **77**, 4391.
- 49 U. Even, J. Magen, J. Friedman and J. Jortner, *J. Chem. Phys.*, 1982, **77**, 4384.

- 50 A. Amirav, M. Sonnenschein and J. Jortner, *J. Chem. Phys.*, 1982, **82**, 4378.
- 51 A. Amirav and J. Jortner, *J. Chem. Phys.*, 1985, **82**, 4378.
- 52 (a) W. Radloff, Th. Freudenberg, H. H. Ritze, V. Stert, F. Noach and I. V. Hertel, *Chem. Phys. Lett.*, 1996, **261**, 301; (b) A. A. Ruth and M. T. Wick, *Chem. Phys. Lett.*, 1997, **266**, 206; (c) M. T. Wick, B. Nickel and A. A. Ruth, *Chem. Phys. Lett.*, 1993, **215**, 243.
- 53 R. Englman and J. Jortner, *Mol. Phys.*, 1970, **18**, 145.
- 54 E. Teller, *Isr. J. Chem.*, 1970, **7**, 227.
- 55 J. Jortner and R. D. Levine, in *Mode Selective Chemistry*, ed. J. Jortner, R. D. Levine and B. Pullman, Kluwer Academic Publishers, Dordrecht, 1991, p. 535.
- 56 A. Amirav and J. Jortner, *Chem. Phys. Lett.*, 1986, **132**, 335.
- 57 A. Amirav, C. Horowitz and J. Jortner, *J. Chem. Phys.*, 1988, **88**, 3092.
- 58 R. Marcus and N. Sutin, *Biochim. Biophys. Acta*, 1985, **811**, 275.
- 59 J. Jortner, M. Bixon, H. Heitele and M. E. Michel-Beyerle, *Chem. Phys. Lett.*, 1992, **197**, 131.
- 60 J. Jortner, M. Bixon, B. Wegewijs, J. W. Verhoeven and R. P. H. Rettschnick, *Chem. Phys. Lett.*, 1993, **205**, 451.
- 61 M. Bixon and J. Jortner, *J. Phys. Chem.*, 1993, **97**, 13061.
- 62 J. Jortner and M. Bixon, *J. Photochem. Photobiol. A*, 1994, **82**, 5.
- 63 A. B. Meyers, *Chem. Rev.*, 1996, **96**, 911.
- 64 J. Cotes, H. Heitele and J. Jortner, *J. Phys. Chem.*, 1994, **98**, 2527.
- 65 B. Wegewijs and J. W. Verhoeven, *Adv. Chem. Phys.*, 1997, in press.
- 66 B. Wegewijs, R. M. Hermant, J. W. Verhoeven, A. G. M. Kunst and R. P. Rettschnick, *Chem. Phys. Lett.*, 1987, **140**, 587.
- 67 B. Wegewijs, A. K. F. Ng, R. P. H. Rettschnick and J. W. Verhoeven, *Chem. Phys. Lett.*, 1992, **200**, 357.
- 68 M. Bixon and J. Jortner, *J. Chem. Phys.*, 1997, **107**, 1470.
- 69 M. Bixon and J. Jortner, to be published.
- 70 M. Bixon and J. Jortner, *J. Chem. Phys.*, 1994, **102**, 5636.
- 71 M. Bixon and J. Jortner, *Mol. Phys.*, 1996, **89**, 373.
- 72 M. Bixon and J. Jortner, *J. Phys. Chem.*, 1996, **100**, 11 914.
- 73 M. Bixon and J. Jortner, *J. Chem. Phys.*, 1997, **107**, 5154.
- 74 F. H. Mies and M. Kraus, *J. Chem. Phys.*, 1966, **45**, 4455.
- 75 I. McLaughlin, S. A. Rice and J. Jortner, *J. Chem. Phys.*, 1968, **49**, 2756.
- 76 I. Schek and J. Jortner, *J. Chem. Phys.*, 1979, **70**, 3016.
- 77 B. Carmeli and A. Nitzan, *J. Chem. Phys.*, 1980, **72**, 2054.
- 78 B. Carmeli, I. Schek, A. Nitzan and J. Jortner, *J. Chem. Phys.*, 1980, **72**, 1928.
- 79 A. Stollow, to be published.
- 80 V. Höfer, I. L. Shumay, Ch. Reus, U. Thomann, W. Wallauer and Th. Fauster, *Science*, 1997, **277**, 1480.
- 81 R. Bersohn and A. H. Zewail, *Ber. Bunsen-Ges. Phys. Chem.*, 1988, **92**, 373.
- 82 R. B. Bernstein and A. H. Zewail, *J. Chem. Phys.*, 1989, **90**, 829.
- 83 J. Jortner and R. D. Levine, *Isr. J. Chem.*, 1990, **30**, 207.
- 84 I. Last, I. Schek and J. Jortner, *J. Chem. Phys.*, 1997, **107**, 6685.
- 85 J. Purnell, E. M. Snyder, S. Wei and A. W. Castleman, *Chem. Phys. Lett.*, 1994, **229**, 333.
- 86 J. Jortner, U. Even, A. Goldberg, I. Schek, T. Raz and R. D. Levine, *Surf. Rev. and Lett.*, 1996, **3**, 263.
- 87 J. Jortner, *J. Chim. Phys.*, 1995, **92**, 205.
- 88 U. Buck and R. Krohne, *Phys. Rev. Lett.*, 1994, **73**, 947.
- 89 A. Goldberg and J. Jortner, *J. Chem. Phys.*, in press.
- 90 I. Schek, T. Raz, R. D. Levine and J. Jortner, *J. Chem. Phys.*, 1995, **101**, 8390.
- 91 R. Zwanzig, A. Zabo and B. Batchi, *Proc. Natl. Acad. Sci. U.S.A.*, 1992, **89**, 20.
- 92 C. Lieman and A. H. Zewail, *Chem. Phys. Lett.*, 1993, **213**, 289.
- 93 J. M. Papanikolas, P. E. Maslen and R. Parson, *J. Chem. Phys.*, 1995, **102**, 2452.
- 94 T. Baumert and G. Gerber, *Adv. At. Mol. Phys.*, 1995, **35**, 163.
- 95 M. Hartmann, R. E. Miller, J. P. Toennies, A. F. Vilesov and G. Benedek, *Phys. Rev. Lett.*, 1996, **76**, 4560.
- 96 N. R. Kestner, J. Logan and J. Jortner, *J. Phys. Chem.*, 1974, **78**, 2148.
- 97 J. Ulstrup and J. Jortner, *J. Chem. Phys.*, 1975, **63**, 4358.
- 98 M. Bixon and J. Jortner, *Chem. Phys.*, 1993, **176**, 467.
- 99 M. Bixon and J. Jortner, *Adv. Chem. Phys.*, in press.
- 100 M. Rosenblit and J. Jortner, *Phys. Rev. Lett.*, 1995, **75**, 4079.
- 101 M. Rosenblit and J. Jortner, *J. Phys. Chem.*, 1997, **101**, 751.
- 102 R. M. Hochstrasser, to be published.
- 103 M. H. Vos, F. Rappaport, J. C. Lambry, J. Breton and J. L. Martin, *Nature (London)* 1993, **363**, 320.
- 104 O. Kühn and V. Sundström, *J. Phys. Chem.*, 1997, **101**, 3422.
- 105 M. Seel, S. Engleitner and W. Zinth, *Chem. Phys. Lett.*, 1997, **275**, 363.

- 106 G. R. Fleming, *Adv. Chem. Phys.*, in press.
- 107 K. Wynne, G. D. Reid and R. M. Hochstrasser, *J. Chem. Phys.*, 1996, **15**, 2287.
- 108 W. H. Zhang, T. Meier, V. Chernyak and S. Mukamel, *Philos. Trans. R. Soc. London*, 1998, **356**, 105.
- 109 M. Bixon, J. Jortner and M. E. Michel-Beyerle, *Chem. Phys.*, 1995, **197**, 389.
- 110 M. E. Beyerle, M. Plato, J. Deisenhofer, H. Michel, M. Bixon and J. Jortner, *Biochim. Biophys. Acta*, 1988, **932**, 52.
- 111 M. E. Michel-Beyerle, private communication and to be published.
- 112 J. Deisenhofer, O. Epp, K. Miki, R. Huber and H. Michel, *Nature (London)*, 1985, **318**, 618.
- 113 N. Haberstadt and K. C. Janda, to be published.
- 114 T. Hertel, E. Konesel, M. Wolf and G. Ertl, *Phys. Rev. Lett.*, 1996, **76**, 535.
- 115 M. Wolf, *Surf. Sci.*, 1997, **377**, 343.
- 116 D. Botkin, J. Glass, D. Chemla, D. F. Ogletree, H. Salmeron and S. Weiss, *Appl. Phys. Lett.*, 1996, **69**, 1321.
- 117 C. A. Coulson, *Rev. Mod. Phys.*, 1960, **32**, 170.

Paper 8/01832D; Received 5th March, 1998